Effects of ensheathing cells transplanted into photochemically damaged spinal cord

Enrique Verdú, Guillermo García-Alías, Joaquim Forés, Graciela Gudiño-Cabrera,[1,2] Vilma C. Muñetón,[1] Manuel Nieto-Sampedro[1] and Xavier Navarro[CA]

Neuroplasticity and Regeneration Group, Department of Cell Biology, Physiology and Immunology, Universitat Autònoma de Barcelona, Edif. M., E-08193 Bellaterra; [1]Neural Plasticity Group, Instituto Cajal, CSIC, Madrid, Spain; [2]Department of Cellular and Molecular Biology, University of Guadalajara, Mexico

[CA]Corresponding Author

Received 2 May 2001; accepted 22 May 2001

Transplantation of olfactory ensheathing cells (OECs) into photochemically damaged rat spinal cord diminished astrocyte reactivity and parenchyma cavitation. The photochemical lesion performed at T12–L1 resulted in severe damage to the spinal cord, so that during the first 15 days postoperation all rats dragged their hindlimbs and did not respond to pinprick. The maximal area and volume of the cystic cavities were lower in transplanted than in non-transplanted rats, not significantly at the T12–L1 lesion site, but significantly at T9–T10 and L4–L6 cord levels. The density of astrocytes in the grey matter was similar at T12–L1 and L4–L6 in non-transplanted and transplanted rats, but lower in the latter at T9–T10 level. However, in non-transplanted rats all astrocytes showed a hypertrophied appearance, with long and robust processes heavily GFAP-positive, and overexpression of proteoglycan inhibitor of neuritogenesis, whereas in transplanted rats only a few astrocytes showed hypertrophy and the majority had short, thin processes. These results indicate that OECs transplanted into damaged adult rat spinal cord exert a neuroprotective role by reducing astrocytic gliosis and cystic cavitation. *NeuroReport* 12:2303–2309 © 2001 Lippincott Williams & Wilkins.

Key words: Astrocyte; Cystic cavity; Ensheathing cells; Photochemical injury; Spinal cord

INTRODUCTION

In the adult CNS, axonal regeneration following injury is influenced by both glial substrates and the extracellular matrix. Following lesions that alter the gross morphology of the CNS, such as transection, compression or photochemical injury, astrocyte proliferation and reactivity contribute to the establishment of a glial scar that can be a physical and chemical barrier to axonal extension [1]. Infusion of trophic factors and cell transplantation (neurons and glial cells) are the main strategies for promoting axonal regeneration in the CNS. Recently, olfactory ensheathing cells (OECs) have been used for promoting axonal regeneration in spinal cord [2–4] and peripheral nerve [5]. OEC transplantation promoted functional recovery after lumbar rhizotomy [6] and spinal cord transection [4].

When a photosensitizing organic dye (Rose Bengal, erythrosin B) is injected into the spinal cord and irradiated with a light beam of appropriate wavelength, the light is absorbed by the dye resulting in free radical production. This causes vascular endothelium dysfunction and platelet aggregation with subsequent vascular occlusion, edema and tissue necrosis [7–11], simulating the secondary response seen after traumatic spinal cord injury [12]. Cystic cavities are formed during the first 14 days after photochemical injury and remain up to 17 months post-injury [9,10]. Schwann cell (SC) grafts implanted into photochemically damaged adult rat spinal cord promote axonal ingrowth at 14 days after implantation with minimal astrocytic gliosis at the interface [13]. These results suggest that SC transplantation into the injured spinal cord may reduce astrocytic gliosis and promote axonal regeneration. However, the beneficial effects of transplanted SCs are restricted to the transplantation area because astrocytes inhibit their migration. In comparison to SCs, OECs secrete similar neurotrophic and neurotropic factors, but are able to migrate long distances in the CNS [14]. In this study we have analyzed the effects of OEC transplants on the astrocytic reaction and size of the cystic cavities formed after photochemical injury of the adult rat spinal cord.

MATERIALS AND METHODS

Primary cultures of OECs from adult (2.5 months old) male Wistar rats were prepared, immunopurified, labeled with PKH26 cell linker (Sigma, St Louis, MO), and stored frozen as described in detail elsewhere [15]. For transplantation, frozen cell vials were thawed at 37°C, washed three times by centrifugation ($200 \times g$, 7 min) in Dulbecco's modified Eagle's medium (DMEM), and the pellet resuspended in the same medium. The cells were transplanted within 2 h of thawing.

Twenty female Sprague–Dawley rats (250–300 g) were anesthetized with sodium pentobarbital (50 mg/kg, i.p.)

and the back of the animal was shaved and disinfected with povidone iodine. The skin and muscles were cut longitudinally and the spinal cord was exposed at T12–L1 by an extensive dorsal laminectomy. The dura was cut and local infiltration with bupivacaine (0.5%) was made to minimize nociceptive input. Rose Bengal (RB; 1.5% in saline; Sigma) was applied directly on the exposed spinal cord for 10 min. The excess dye was then removed by a double saline rinse. Illumination was performed by means of two optic fibers positioned 10 mm above the spinal cord [16]. The fibers were connected to a cold light source equipped with a 150 W halogen bulb (Raypa, Barcelona, Spain). Spinal cord was illuminated at maximal nominal power for 5 min. Ten rats then received a bilateral injection of a suspension of OECs (60 000 in 3 µl DMEM) into each spinal cord level from T12 to L1 (group RB5 + EC). The cell suspension was applied through a glass micropipette by means of repeated 20 ms air pulses of 10 psi (Picospritzer II, General Valve, Fairfield, NJ) [6]. A control group (group RB5) was formed by 10 non-transplanted rats. Finally, the wound was sutured with 5-0 silk thread in the muscular plane and the skin was closed with small clips and disinfected. The animals were kept in a warm environment until full recovery and were given amitriptyline (150 µg/ml) in their drinking water to prevent autotomy [6].

Functional tests were performed before operation and daily up to 15 days post-operation (dpo). Locomotor activity was evaluated using the open-field walking scoring system of Cheng *et al*. [17], which measures the locomotor ability over 15 min. One animal at a time was allowed to move freely inside a plastic tray ($60 \times 90 \times 24$ cm) and the locomotor function was scored according to a modified Tarlov scale: no spontaneous movement (0), movement in the hip or knee but not ankle (1), movement of the limb in the all three major joints (2), active support and an uncoordinated gait or occasional short bouts of coordinated gait (3), coordination of forelimbs and hindlimbs in gait, including some walking on knuckles or the medial surface of the foot or a few toe drags (4), and normal gait (5). Nociceptive sensitivity was tested by light pricking with a needle on the plantar surface of both hindpaws. The normal response was vocalization and withdrawal of the paw and the pinprick score assigned ranged from no response (0) to normal reaction (2).

Fifteen days after injury, all animals were anesthetized and perfused transcardially with 4% paraformaldehyde in phosphate-buffered saline (PBS, 0.1 M, pH 7.4). The spinal cords were removed, fixed in the same solution for 24 h and divided into three blocks identified as T9–T10, T12–L1 and L4–L6. Blocks were postfixed in Zamboni's fixative solution for 24 h, then cryoprotected in PBS containing 20% sucrose and stored at 4°C. Spinal cord blocks were sectioned in a cryotome (Reichert). Transverse sections (100 µm) were washed free-floating in PBS with 0.3% Triton X-100 (Fluka) and 1% normal goat serum (NGS) (ICN Pharmaceuticals) for 1 h and incubated with rabbit antiserum to glial fibrillary acidic protein (GFAP; 1:200, Chemicon) overnight at 4°C, and with mouse antiserum to proteoglycan [18] (3PE8; 1:400) for 48 h at 4°C. After washing, the sections were incubated overnight at 4°C with Cy2- or Cy3-labelled donkey anti-rabbit or anti-mouse immunoglobulin G (1:200, Jackson Immunoresearch). Following additional washes, sections were mounted on gelatin-coated slides, dehydrated in ethanol and mounted with dextropropoxyphene (DPX, Fluka). Samples were viewed under an Olympus BX-40 microscope equipped for epifluorescence [6]. Low power magnification (×10) images of spinal cord sections were taken with the aid of a digital camera (Olympus DP20) attached to the microscope and analyzed using NIH Image software. The cross-sectional area of the cystic cavity was measured in sections of the three blocks. The volume of the lesion cavity at each spinal cord level was calculated assuming that the shape of the lesion resembled a truncated cone, as $V = L/3 \times (A + a + a')$, where L is the length of the spinal cord block and A, a and a′ are the maximal, minimum and intermediate areas of the cystic cavities, respectively. The density of astrocytes (cells/mm^2) was calculated from images of spinal cord sections collected with a confocal imaging system (Leica TCS-4D). Using NIH Image software, the cell bodies of GFAP-immunoreactive (-ir) astrocytes were counted on at least five sections per animal and spinal block in a 0.07 mm^2 area of the grey matter [19].

The experimental protocols adhered to the recommendations of the European Union and the US Department of Health for the care and use of laboratory animals and were approved by the ethical committees of our Institutions. Functional and histological measurements were performed in a blind manner. All results are shown as mean and SEM. Statistical comparisons between control and transplanted groups were made using Kruskal–Wallis and Mann–Whitney U tests. Differences were considered significant at $p < 0.05$.

RESULTS

Before the spinal cord lesion all rats showed normal gait (score 5) and nociceptive responses (score 2). On the day following injury, all the rats dragged the hindpaws and did not show any response to pinpricking the paw. At 7 dpo only two of the 10 rats in each group showed mild responses to pinprick and in open field walking. The score to pinprick averaged 0.33 ± 0.18 and 0.33 ± 0.16 in groups RB5 and RB5+GE, respectively, whereas the mean score of open field walking was 0.11 ± 0.07 for both groups. During the second week, slight spontaneous recovery was observed. By 15 dpo, the mean values increased to scores of 1.17 ± 0.23 and 1.28 ± 0.23 for pinprick, and 0.83 ± 0.31 and 0.72 ± 0.19 for open field walking in non-transplanted and transplanted rats, respectively ($p > 0.05$). At the last test, five of 10 rats of both experimental groups showed positive responses to pinprick and hip and/or knee movements.

In spinal cord sections at T12–L1 of group RB5 rats a cavity surrounded by GFAP-ir cells was observed affecting the dorsal and dorsolateral funiculi and the grey matter, whereas the ventrolateral and ventromedial funiculi were preserved (Fig. 1a). The cavity extended longitudinally over several spinal segments. In sections taken at T9–T10 the cavity involved mainly the dorsal columns spreading to the central canal (Fig. 1c). A similar pattern was found in spinal cord sections of L4–L6. In transplanted rats (group RB5 + EC) a cavity involving the dorsal funiculus including the dorsal horns was observed in sections of T12–L1 (Fig. 1b). A small cavity was seen in sections taken at T9–T10 and L4–L6 levels, partially affecting the dorsal

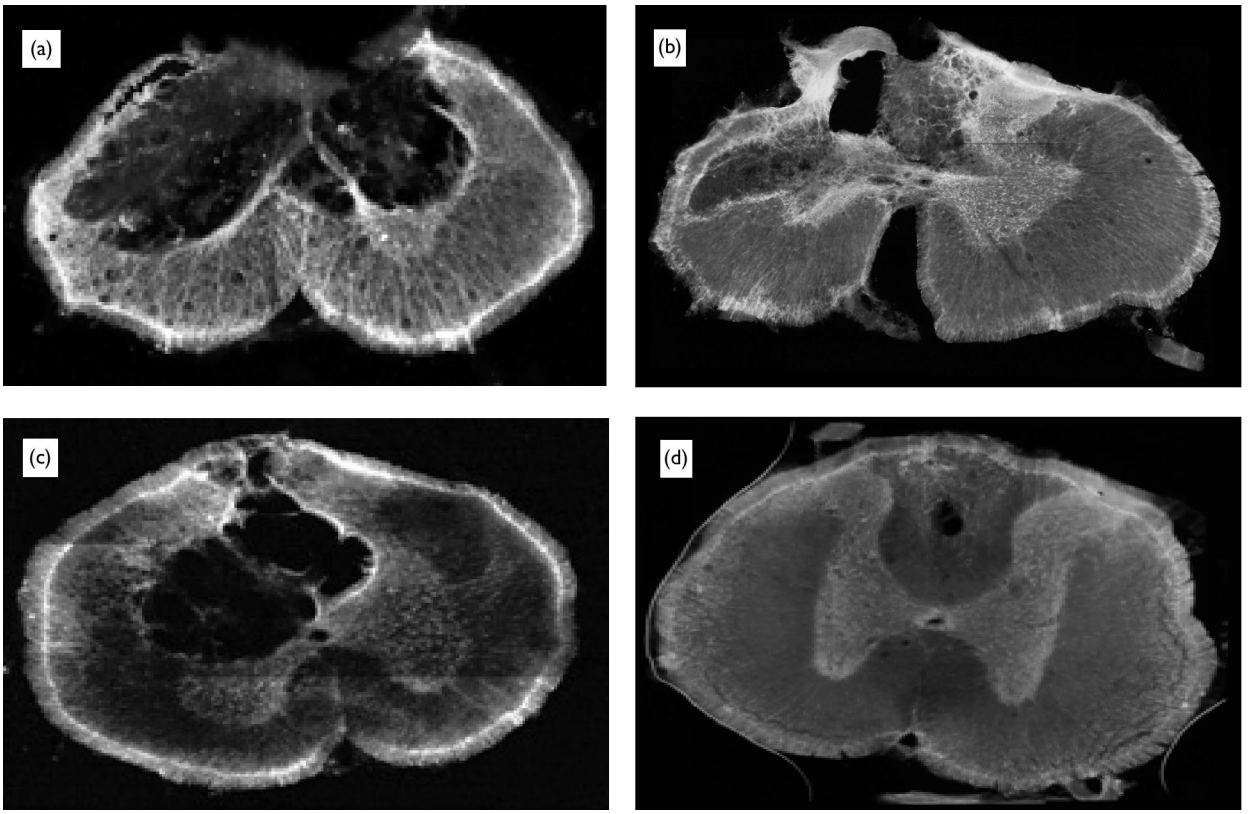

Fig. 1. Spinal cord sections immunostained against GFAP from non-transplanted (**a**,**c**) and transplanted (**b**,**d**) rats taken at the injured segments T12–L1 (a,b) and at rostral segments T9–T10 (c,d). ×25.

funiculus (Fig. 1d). The maximal area of the cystic cavity measured in all spinal cord blocks and the calculated volume of the cavity were lower in group RB5 + EC than in group RB5, with significant differences found at T9–T10 and L4–L6 levels for both parameters (Table 1).

The density of astrocytes (GFAP-ir cells) in the grey matter of preserved spinal cord areas was similar in non-transplanted and in transplanted rats at T12–L1 and L4–L6 levels, but lower at T9–T10 in transplanted rats (Table 1). In spinal cord sections from rats of group RB5, all astrocytes showed a hypertrophied appearance, with long and robust processes extending in all directions and heavily stained for GFAP and 3PE8 (Fig. 2a,b). These reactive astrocytes were observed in dorsal and ventral horns of the three spinal cord blocks analyzed. In transplanted rats, few astrocytes showed a hypertrophied appearance, and most showed intensely GFAP-stained cell bodies with short and thin processes. A similar appearance was observed when spinal cord sections were stained against proteoglycan (3PE8; Fig. 2c,d). Reactive hypertrophied astrocytes were observed in dorsal and ventral horns at the lesion site, but very few reactive astrocytes were seen in rostral (T9–T10) and caudal (L4–L6) cord sections.

OECs pre-labeled with PKH26, identified by their red fluorescence, were observed surrounding the necrotic dorsal cavity (Fig. 3), in the grey matter near the central canal, but also spread through the dorsal and ventral grey matter.

Table 1. Immunohistochemical results from transplanted (RB5 + EC) and non-transplanted (RB5) spinal cords.

Parameter	Group	T9–T10	T12–L1	L4–L6
Maximal area of cavity (mm^2)	RB5	0.35 ± 0.15	2.25 ± 0.70	0.15 ± 0.06
	RB5 + EC	0.05 ± 0.02	1.82 ± 0.52	0.02 ± 0.02
	p	0.023	0.566	0.040
Volume of cavity (mm^3)	RB5	1.21 ± 0.60	16.74 ± 4.22	0.57 ± 0.22
	RB5 + EC	0.17 ± 0.08	12.68 ± 3.67	0.08 ± 0.08
	p	0.002	0.269	0.040
Density (GFAP-ir cells/mm^2)	RB5	297.5 ± 17.6	308.4 ± 32.6	245.1 ± 33.3
	RB5 + EC	230.9 ± 26.8	303.9 ± 40.1	279.3 ± 32.3
	p	0.050	0.847	0.855

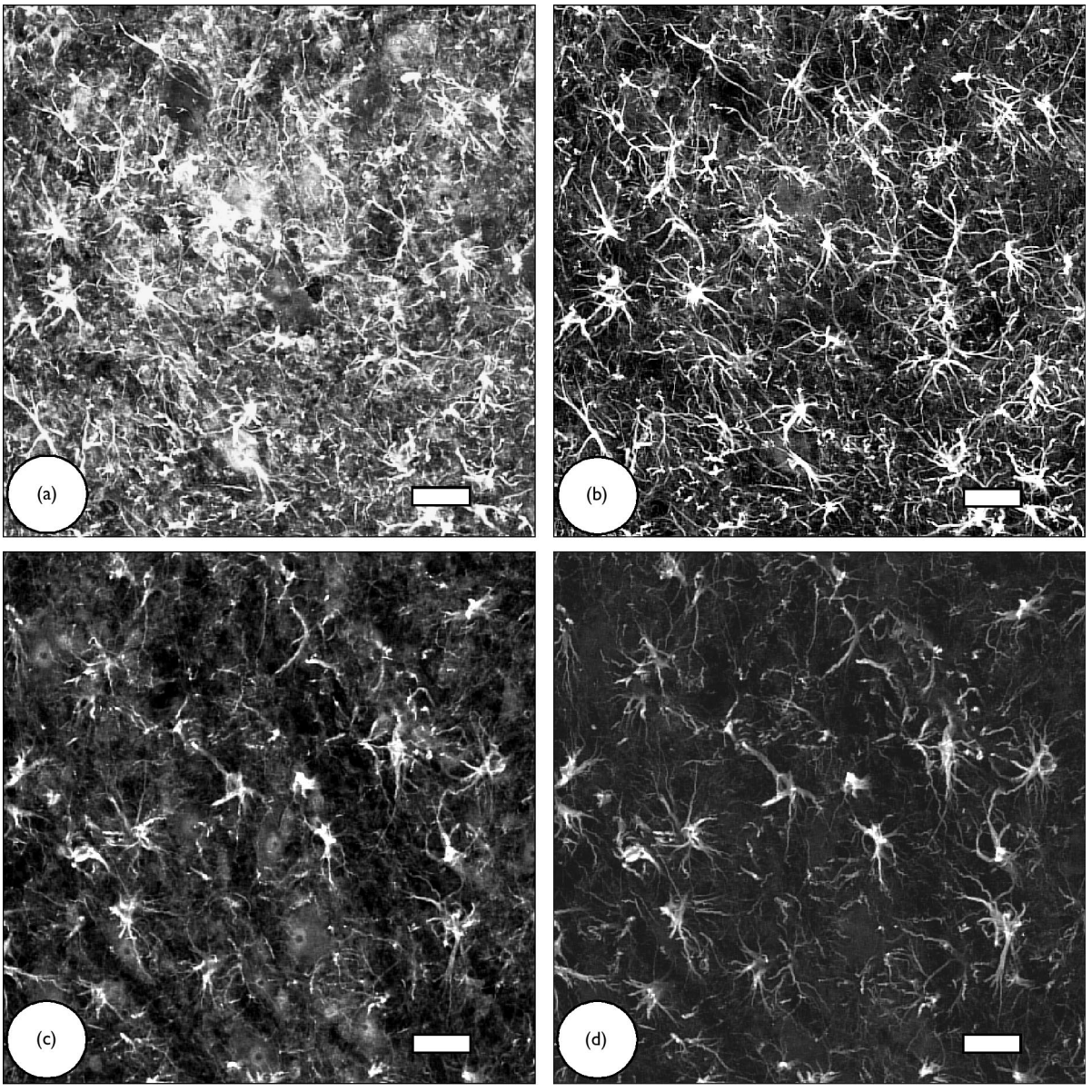

Fig. 2. Confocal images of astrocytes immunolabelled against GFAP (**a**,**c**) and against 3PE8 (**b**,**d**) in the grey matter of non-transplanted (a,b) and OEC transplanted (c, d) rats. Note co-localization of GFAP and 3PE8, and the clear difference in size and processes between astrocytes of non-transplanted and transplanted cords. Bar = 25 μm.

OECs were more abundant in sections at the T12–L1 levels and in the grey than in the white matter of rostral and caudal spinal cord blocks (Fig. 3).

DISCUSSION

The results of this study show that OECs transplanted into photochemically damaged adult rat spinal cord exert a neuroprotective role by reducing astrocytic gliosis and cystic cavitation during the first 15 days postlesion. Transplanted spinal cords showed a lower cystic cavity volume and reduced astrocytic reactivity with respect to non-transplanted cords.

Anisomorphic lesions of the CNS, typically caused by mechanical trauma, disrupt the glia limitans and the blood–brain barrier at the injury site. Vascular breakage and vasospasm cause ischemia, hypoxia and hypoglycemia, together with invasion of the injury area by blood cells and serum proteins. During the first 48 h after anisomorphic injury, edema in grey and white matter, uniform necrosis and myelin degeneration, blood-derived macrophages, and degenerating myelin and other cell debris are observed at the lesion site [20]. Photochemical injury of the adult spinal cord causes plasma extravasation at 1 h post-lesion, and by 48 h the tissue is edematous with disintegrated tissue and increased intercellular space. GFAP-ir cells were observed at 24 h post-lesion, but they were more abundant at the border of the cavities at 14 days post-injury [11]. In an ultrastructural study, Bunge *et al*. [10] showed that near the lesion cavity perimeter, axons were swollen and only partly encased in myelin. They

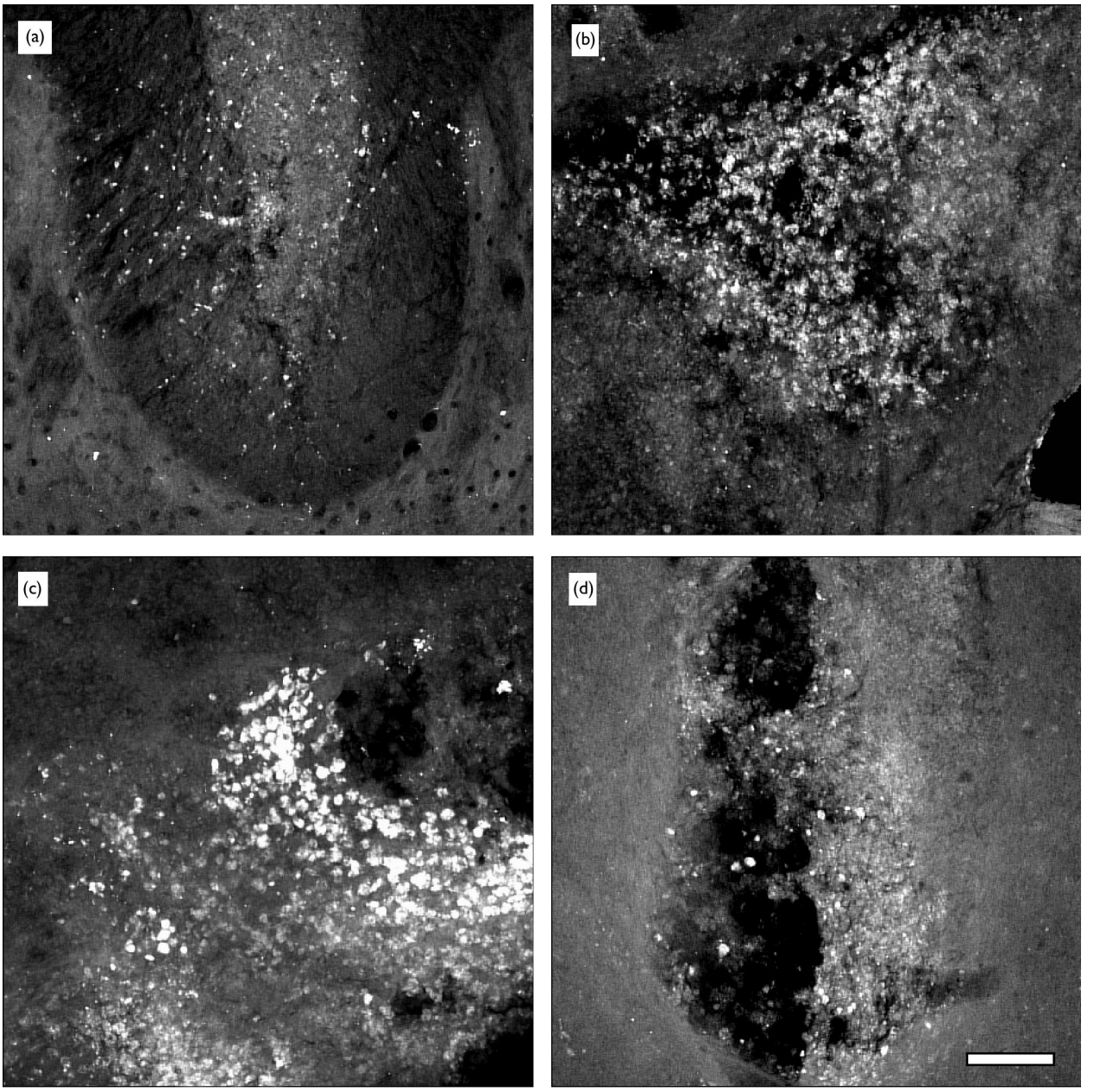

Fig. 3. Confocal images of spinal cord sections from transplanted rats at T9–T10 (**a**,**b**) T12–L1 (**c**) and at L4–L6 (**d**), showing pre-labeled PKH26 ensheathing glial cells (white points). OECs are observed in white matter of the dorsal funiculus (a) and in the grey matter near central canal (b) and around cystic cavities (c,d). Bar = 100 μm.

contained aggregates of organelles in various stages of deterioration. Macrophages were rare at 2 days but were increased in number in the lesion cavity by 5 days [10]. All these findings clearly demonstrated that the photochemically induced spinal cord injury may be considered as a model of anisomorphic lesion.

Following the method first described by Watson and coworkers [7], RB was injected into the tail vein over a 5 min period to yield a body concentration of 40 mg/kg. Immediately following the injection, the spinal cord (at T8) was irradiated by means of a xenon laser lamp that produced a green beam centered at 560 nm. When the spinal cord was irradiated for 5 min, histopathological examination revealed ischemic necrosis involving all the white matter tracts except the ventrolateral funiculi and the ventromedial tracts of the anterior funiculi. This region contained areas of extensive demyelination with vacuoles interspersed among regions of normally appearing myelinated axons. Functionally, these animals showed a neurological deficit of about 75% at 1 week. At this time there was no response to pain, and the rats showed impaired motor function [8]. These findings are similar to those observed in the present study, where RB was applied topically on the spinal cord dorsal surface and irradiated with cold light.

The abolished functional responses seen during the first week post-lesion and the minimal spontaneous recovery by 15 dpo observed in the present study are similar to those observed after severe contusion or complete spinal cord transection [21]. Immediately after such spinal cord lesions, rats exhibit flaccid paralysis that persists for 3–7 days. Between 7 days and 6 weeks post-lesion, most rats recover only slight hindlimb joint movements [21]. Our functional results confirm that the method used in the present study may be considered as a severe model of spinal cord injury.

Cystic cavitation is an usual feature of anisomorphic spinal cord lesions [10,12,21], including photochemical injury [9–13]. In a light and electron microscopy study, Bunge *et al*. [10] found the first cystic cavities at 2 days after photochemically induced spinal cord injury. The area of cystic cavities increased during the first 2 weeks post-lesion but did not change later up to 56 days post-lesion. Evidence of axonal regrowth around the lesion was found between 2 and 6 months, a period when the lesion cavities diminished in size [10,12]. Spontaneous axonal regeneration for short distances has also been described after spinal cord compression. Of interest is that the regenerating axons circumvented the fluid-filled cysts formed at the rostral and caudal borders [22]. These findings indicate that 2 weeks post-lesion is a critical period for development of cystic cavities, and regenerating axons appear in the lesion site later, when the size of lesion cavities is reduced. The reduction in volume of the cystic cavity found at 15 dpo in the OECs transplanted rats is a clear indication of reduced damage and thus protection to the spinal cord tissue, thus providing a better substrate for eventual axonal regeneration. Therefore, the transplanted OECs exerted a neuroprotective role, reducing the loss of neurons and glial cells.

Astrocytes become reactive in response to anisomorphic lesions of the CNS. Hallmarks of astrocyte reactivity include hypertrophy of the cell body, increased arborization of processes and up-regulation of intermediate filaments such as GFAP and vimentin [23]. The most important cell type in CNS scars is the astrocyte, with additional contributions of fibroblasts, microglial cells, macrophages, connective tissue, and during scar formation, inflammatory cells [20]. The glial scar surrounding cystic cavities in the CNS parenchyma has been observed in all anisomorphic lesions, including the photochemically induced spinal cord lesion [10,11]. The end feet of hypertrophied astrocytes form multilayered interfaces between necrotic and intact neural tissue [10,20]. Reactive astrocytes produce chondroitin sulphate proteoglycans (CS-PGs) that are localized into the glial scar [24,25]. *In vitro* studies indicate that CS-PGs can inhibit neurite outgrowth [18,26]. Recently, Lakatos *et al*. [27] reported that the number of astrocytes expressing CS-PGs was increased when astrocytes were co-cultured with SCs but not when astrocytes were grown with OECs. In the present study we found that *in vivo*, OECs are also able to reduce the astrogliotic response. The astrocytes observed in spinal cord sections from OECs transplanted rats were less hypertrophied and had lower immunoreactivity to GFAP and CS-PGs than in non-transplanted animals. Therefore, transplanted OECs were able to reduce the neurite inhibitory factors associated with astrogliosis.

Several studies have reported that transplanted OECs promote axonal regeneration in the spinal cord [2–4,6]. Regeneration of corticospinal axons was observed guided by transplanted OECs in a focal lesion of the corticospinal tract. The cut axons elongated along the axis of the corticospinal tract as single sprouts, which by 3 weeks post-transplant crossed the full length of the lesioned area and reentered the caudal part of the host corticospinal tract [3]. Eight months after complete cord transection, corticospinal, noradrenergic and serotoninergic axons were observed in the distal spinal cord stumps of animals receiving OECs transplants [4]. These findings suggest that, in the short term, transplanted OECs create an appropriate environment that later allows for effective axonal regeneration. OECs produce a variety of adhesion molecules and growth factors such as BDNF, PDGF, NGF, neurotrophin 3 (NT-3) and neurotrophin 4 (NT-4). In addition to neurotrophic factors, OECs express laminin, L1, fibronectin, S100, neuropeptide Y, glial-derived nexin and neural cell adhesion molecule (N-CAM). OECs are also immunoreactive against the low-affinity NGF receptor (p75) [14]. Neurotrophins secreted by OECs interact with neurons to promote survival and axonal regeneration, but may also interact with glial cells to induce secretion of higher quantities of neurotrophic factors, and probably to reduce their reactivity. Reactive astrocytes and microglia express tyrosine kinase receptors (trk-A, trk-B, trk-C), and BDNF, NGF, NT-3 and NT-4 bind with these receptors modulating their biochemical activity [28,29].

OECs are able to migrate long distances in the CNS [3,4,15] and their effects are not restricted to the site of transplantation. In the present study, OECs transplanted at the injured T12–L1 spinal cord segments, were found by 15 dpo in considerable numbers at T9 and L4. Thus, they were able to survive and migrate in spite of the difference in strain between donor and host animals. Using co-cultures of astrocytes and OECs, Lakatos and co-workers [27] have reported that OECs migrate across astrocyte monolayers, as well as through a three-dimensional astrocyte matrix, such as they confront within the CNS parenchyma or at the glial scar.

CONCLUSION

This study demonstrates that OECs transplanted into a photochemical injury of adult rat spinal cord help to reduce astrocytic gliosis and cystic cavitation during the first 2 weeks post-lesion. These effects may be attributed to their ability to migrate within the parenchyma of the CNS and secrete neurotrophic factors and/or other factors that reduce astrocytic and microglial reaction. The decrease in the inhibitory properties of the microenvironment created after a CNS injury and the permissive environment created by OECs may promote axonal regeneration at a later time.

REFERENCES

1. Hatten ME, Liem RK, Shelanski ML *et al. Glia* **4**, 233–243 (1991).
2. Ramón-Cueto A and Nieto-Sampedro M. *Exp Neurol* **127**, 232–244 (1994).
3. Li Y, Field PM and Raisman G. *J Neurosci* **18**, 10514–10524 (1998).
4. Ramón-Cueto A, Cordero MI, Santos-Benito FF *et al*. *Neuron* **25**, 425–435 (2000).
5. Verdú E, Navarro X, Gudiño-Cabrera G *et al*. *Neuroreport* **10**, 1097–1101 (1999).

6. Navarro X, Valero A, Gudiño G *et al. Ann Neurol* **45**, 207–215 (1999).
7. Watson BD, Prado R, Dietrich WD *et al. Brain Res* **367**, 296–300 (1986).
8. Prado R, Dietrich WD, Watson BD *et al. J Neurosurg* **67**, 745–753 (1987).
9. Cameron T, Prado R, Watson BD *et al. Exp Neurol* **109**, 214–223 (1990).
10. Bunge MB, Holets VR, Bates ML *et al. Exp Neurol* **127**, 76–93 (1994).
11. Von Euler M, Sunström E and Seiger Å. *Acta Neuropathol* **94**, 232–239 (1997).
12. Watson BD, Holets VR, Prado R *et al. Neuroprotocols* **3**, 3–15 (1993).
13. Paino CL and Bunge MB. *Exp Neurol* **114**, 254–257 (1991).
14. Ramón-Cueto A and Avila J. *Brain Res Bull* **46**, 175–187 (1998).
15. Gudiño-Cabrera G and Nieto-Sampedro M. *Restor Neurol Neurosci* **10**, 25–34 (1996).
16. Van Reempts J and Borgers M. *Histol Histopathol* **9**, 185–195 (1994).
17. Cheng H, Cao Y and Olson L. *Science* **273**, 510–513 (1996).
18. Bovolenta P, Fernaud-Espinosa I, Méndez-Otero R *et al. Eur J Neurosci* **9**, 977–989 (1997).
19. Baldwin SA, Broderick R, Blades DA *et al. J Neurotrauma* **15**, 1015–1026 (1998).
20. Schwab ME and Bartholdi D. *Physiol Rev* **76**, 319–370 (1996).
21. Basso DM, Beattie MS and Bresnahan JC. *Exp Neurol* **139**, 244–256 (1997).
22. Brook GA, Plate D, Franzen R *et al. J Neurosci Res* **53**, 51–65 (1998).
23. Eng LF, Yu ACH and Lee YL. *Prog Brain Res* **94**, 353–365 (1992).
24. Lemons ML, Howland DR and Anderson DK. *Exp Neurol* **160**, 51–65 (1999).
25. McKeon RJ, Jurynec MJ and Buck CR. *J Neurosci* **19**, 10778–10788 (1999).
26. Bovolenta P, Wandosell F and Nieto-Sampedro M. *Eur J Neurosci* **5**, 454–465 (1993).
27. Lakatos A, Franklin RJM and Barnett SC. *Glia* **32**, 214–225 (2000).
28. Althaus HH and Richter-Landsberg C. *Int Rev Cytol* **197**, 203–277 (2000).
29. Gehrmann J, Matsumoto Y and Kreutzberg GW. *Brain Res Rev* **20**, 269–287 (1995).

Acknowledgements: This research was supported by grants from the FISSS (00/0031) and Societat Catalana de Neurologia-Fundació Uriach, Spain. GG-C. was the recipient of fellowship J_33999N (Mexico).

FUNCTIONAL CHANGES IN THE SPINAL CORD OF THE RAT CAUSED BY INJURIES IN THE THORACIC OR LUMBAR SPINAL SEGMENTS

Guillermo García-Alías[1] Rubén López-Vales[1], Joaquim Forés, [1,2]; Xavier Navarro[1], and Enrique Verdú[1]

[1]Neuroplasticity and Regeneration Group, Institute of Neurosciences and Department of Cell Biology, Physiology and Immunology, Universitat Autònoma de Barcelona, Bellaterra, and [2] Hand Unit, Hospital Clínic i Provincial de Barcelona, Barcelona, Spain.

We have investigated the motor functional changes in the spinal cord following injuries made at T8 or L2 spinal cord segments of the rat. Rose bengal was topically applied to the spinal cords of the animals and afterwards irradiated for 2.5 minutes with a light source. L2 injured animals presented gross locomotor deficits in the BBB open-field scale test, a reduction of the M- and H-response of the distal hindlimb musculature after stimulation of the sciatic nerve, and a strong reduction of the motor evoked potentials (MEPs). T8 injured animals showed mild deficits in locomotion with normal M-response, low MEPs responses but high H-reponse. A reduction in the number of cresyl violet stained and CGRP immunoreactive L4-L5 motoneurons were seen in the T8 and L2 injured groups with respect to unoperated rats.

INTRODUCTION

Traumatic spinal cord injuries result in the death of grey matter neurons and in the disruption of spinal tracts at the site of injury. As a result of the insult, patients lose motor, sensory and autonomic control of the segments of the body below the injury. Patients do not spontaneosly recover and therefore, these deficits persists along their whole lifespan [1] . To achieve the restoration of locomotion, different experimental approaches are being investigated. Cell grafting, neurotrophic factor delivery, growth inhibitor blockade, and intracellular signaling manipulation are some examples of approaches developed to promote axon regeneration across the site of injury [5] . Alternatively, the use of rehabilitation therapies such as drug administration, treadmill locomotor training or electrical stimulation, improves locomotion by enhancing the function of the preserved CNS circuitry [16] . Allthough these therapies are still far away from clinical application, recent studies in animal models and in human clinical trials have shown the possibilities of these interventions in the future.

However, in the majority of experimental studies, the spinal cord injuries have been done at mid thoracic spinal cord segments, while in few studies the lesion have involved the lumbar enlargement of the spinal cord. It is well established that the degree of neurological deficits developed after an injury depend on various parameters, which includes the area of spared parenchyma, the nature of the spinal tracts affected and the anatomical location of the injury [7] . In humans, spinal cord trauma frequently affects the cervical or lumbar vertebrae. Injuries at the lower cervical spinal cord causes paralysis affecting upper and lower extremities, thorax and abdomen; whereas dorsolumbar accidents induce paralysis prefereable of lower extremities [1] . Animals with injuries at the rostral enlargement present dramatic loss of their locomotor abilities [11, 19] . Although the main cause of these disabilities is the disruption of the central pattern generator of locomotion [11] , located in the gray substance of L1-L2 spinal segments [3] , little is known about the changes induced in the lumbar pool of motoneurons. The aim of this work has been to compare functional and morphological changes in the lumbar motorneuron pool induced by injuries produced to the L2 spinal cord segment, or distally on the mid thoracic T8 segment

Ten adult female Sprague-Dawley rats (200-250g) were anaesthetised with sodium pentobarbital (50 mg/kg, i.p.). Laminectomy of the T8 (n= 5, group iT8) or T13 (n= 5, group iL2) vertebrae exposed the spinal cord. Rose Bengal (RB;1.5% in saline solution; Sigma) was topically applied on the dorsal surface of the spinal cord for 10 minutes. The excess dye was removed by saline rinse, and the spinal cord was irradiated with an optic fiber connected to a halogen lamp equipped with a 150-W Xenophot halogen bulb (EFP 64634 HXL, OSRAM, Germany). All the spinal cords were illuminated with an intensity of 80 kLux for 2.5 minutes, controlled by means of a luxometer [20] . Finally, the wound was sutured with a 5-0 silk thread in the muscular plane and the skin was closed with small clips and disinfected. Rats were kept in a warm environment, housed two per cage, exposed to a 12-h light/dark cycle, and had free access to food and water. Five unoperated animals were used as the control group (group CNT).

Gross motor behaviour was evaluated before the surgery and on post opertative days (dpo) 3, 5, 7, 9, 11 and 14 with the open field locomotor test. The animals were placed individually in the middle of a circular enclosure and allowed to move freely for 5 minutes. Two observers evaluated and scored the degree of the animals hindlimbs performance, according to the BBB-scale ranged from 0 (no movement) to 21 (normal movement) developed by Basso, Beattie and Bresnahan (BBB-scale) [2] .

Electrophysiological tests were performed bilaterally on both hindlimbs before the injury and at 14 dpo. The animals were anaesthetised with pentobarbital and placed prone over a warmed flat coil controlled by a hot water circulating pump to maintain skin temperature above 32° C. Motor evoked potentials (MEPs) were elicited by transcranial stimulation with two needle electrodes placed subcutaneously over the skull, the anode over the sensorimotor cortex and the cathode on the hard palate [8] . Single electrical pulses of 25 mA intensity and 100 µ s duration were applied, and the MEPs were recorded with monopolar needle electrodes from the tibialis anterior (TA), gastrocnemius (GM) and plantar (PL) muscles. The signals were amplified, filtered (bandpass 1-5000 Hz) and displayed on oscilloscope (Sapphyre 4ME, Vickers) to measure the latency to the onset of the wave and the amplitude from the onset to the peak of the negative deflection. To ensure reproducibility, at least five consecutive recordings were measured, with a time interval of 30 seconds between stimuli, and the recording with the highest amplitude used for analysis [8] .

Motor nerve conduction studies were performed by the stimulation of the sciatic nerve by single electrical pulses (0,1 ms duration and supramaximal intensity) delivered by monopolar needles inserted percutaneously at the sciatic notch. The compound muscle action potentials (CMAPs) of the TA, GM and PL muscles were recorded during 20 ms by means of needle electrodes, the active electrode inserted on the belly of the muscle and the reference at the second toe, and displayed in the oscilloscope. The H wave, the electrical analogue of the stretch reflex, is elicited by electrical stimulation of large myelinated afferent fibers, and recorded as a late response in the motor nerve conduction test. The latency from stimulus to the negative peak and the amplitude from the onset to the peak of the M and H waves were measured [8] . The ratio of H/M maximal amplitudes was calculated, as it provides an index of the proportion of motoneurones recruited via monosynaptic reflex relative to the total motoneuronal pool [17] . To ensure reproducibility in all the electrophysiological tests, the recording needles were placed under microscopic magnification to secure the same placement in all animals guided by anatomical landmarks.

At the end of the last electrophysiological evaluation the animals were anaesthetised with sodium pentobarbital (40 mg/kg i.p.) and perfused transcardially with 4% paraformaldehyde in phosphate-buffer (PB; 0.1M, pH 7.4). The T8, L2 and L4-L5 spinal cord segments were identified and dissected, fixed over night in the same solution and stored in a cryoprotection solution (30% sucrose in PB) at 4°C. Transverse sections (40 µ m) of the lesioned spinal cord segment (T8 or L2) of the corresponding animals were serially sectioned

with a cryostat, and stained with cresyl violet. In addition, transverse sections from the L4-L5 spinal cord segment of all the animals were also serially cutted with a cryostat (40µ m). Alternate sections were collected, and stained with cresyl violet or processed by immunohistochemical techniques against Calcitonin Gen-Related Peptide (CGRP). Free-floating spinal sections were washed for 1 h, in phosphate-buffer saline (PBS; 0.1M, pH 7.4) with 0.3% Triton-X-100 (Fluka) and 1% fetal calf serum (Biological Industries, Israel). Then, incubated with rabbit primary antiserum to CGRP (1:1000, Chemicon). After several washes, the sections were incubated with a secondary antiserum donkey anti-rabbit Cy2 labeled immunoglobulin G (1:200; Jackson Immunoresearch), overnight at 4°C. Following additional washes, sections were mounted on gelatin coated slides, dehydrated in ethanol and mounted with dextropropoxyphene (DPX, Fluka). Negative controls were done without the application of the primary antibody, and processed as described above. Samples were viewed under a microscope equipped for epifluorescence using the appropriate filter. Low power magnification (x4) images of T8 and L2 spinal cord sections were taken with the aid of a digital camera attached to the microscope, and the preserved spinal cord parenchyma was quantified using NIH Image software [19, 20] . Spinal cord section from L4-L5 segments were used for counting both CGRP-immunoreactive and cresyl violet stained somatas located in ventral horns [20] .

All functional, electrophysiological and histological measurements were performed in a blind manner. Neurological and histological results are shown as mean ± SEM. Electrophysiological results were expressed as the percentage with respect to preoperative values, and the area of preserved parenchyma was normalized respect to the area of the corresponding spinal cord segments of the CNT animals. The results were compared between groups by non-parametrics tests (Kruskal-Wallis and Mann-Whitney U). Differences were considered significant if $p< 0.05$. The experimental protocols adhered to the recommendations of the European Union and the US Department of Health for the care and use of laboratory animals and were approved by the Ethical Committees of our institution.

RESULTS

Figure 1A shows the averaged BBB-scores over time. All animals from CNT group showed normal locomotion during the 14 days of evaluation (scored 21). At 3 dpo, the animals of iT8 and iL2 groups presented locomotor deficits, with an averaged BBB-score of 17.0 ± 1.1 and 0.0 ± 0.1, respectively. Over the course of several days the animals of both experimental groups partially recovered their locomotor habilities, and by 14 dpo the mean BBB-scores were 18.0 ± 0.6 and 10.0 ± 2.8 in the same experimental groups, respectively. Significant differences were found between the three groups (Fig 1A).

After the spinal cord injury, the amplitude of MEPs decreased significantly in iT8 and iL2 groups with respect to unoperated animals (CNT group). No significative differences were seen in the latency of MEPs between iT8 and CNT groups, whereas the latency of MEPs was significantly larger in iL2 group in comparison with iT8 and CNT groups (Table 1). In addition, the CMAP amplitude values were similar in iT8 and CNT groups, whereas decreased significantly in iL2 with respect to iT8 and CNT groups. No significative differences were seen in the CMAP latency for all muscles tested (Table 1). Finally, the percentage of the H/M ratio was significantly higher in injured than control groups (Table 1).

Transverse sections of the injured spinal segments showed that the lesion partially affected to the dorsal lateral area of the spinal cord, including the dorsal columns, the dorsal horns and the dorsal aspect of the lateral funiculus. The spinal cord also presented microcavitations in the grey matter, including ventral horns (Fig 2). In both experimental groups, the ventral horns, the lateral and ventral funiculi were preserved. The percentage of spared spinal cord parenchyma was 100 ± 0, 89 ± 1 and 79 ± 3, in the CNT, iT8 and iL2 groups, respectively. Significant differences were found between iT8 and iL2 respect to the CNT group ($p< 0.05$), but not between the iT8 and iL2 groups.

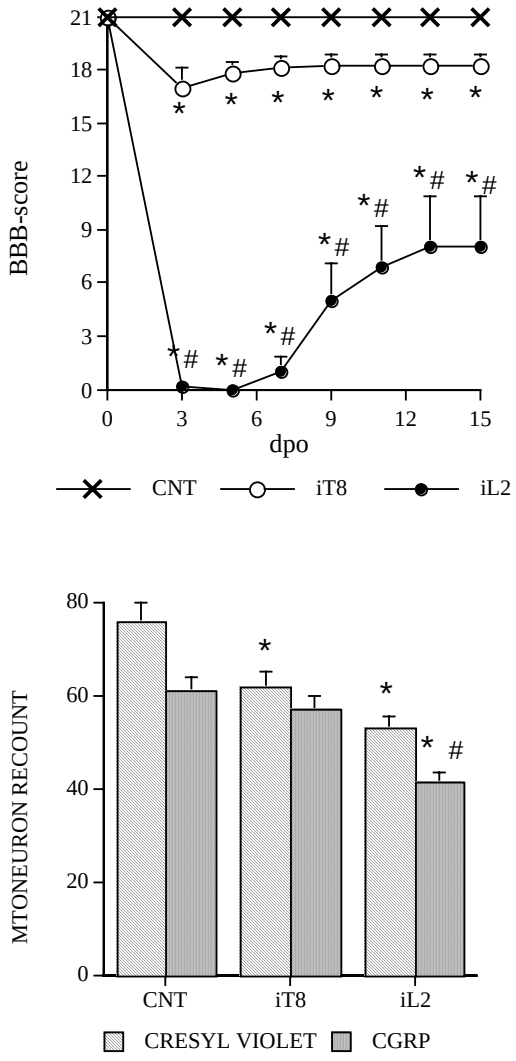

Figure 1. (A) Open field walking scores, evaluated by the BBB-scale over time in the experimental groups studied. (B) Histogram representation of the number of cresyl violet and CGRP positive cells counted in in the VII laminae of the L4-L5 spinal cord segments. (+) p< 0.05 vs CNT group, (#) p < 0.05 C vs iT8 group

The number of cresyl violet and CGRP stained motoneurons in the L4-L5 spinal segments were significant lower in both injured groups compared to the control group (Fig 1B). CGRP immunostained neurons located in laminae VIII had variable labeling intensity. These neurons showed a big soma and their immunostaining pattern was in the form of punctuated granules, which filled the perinuclear cytoplasm. Cresyl violet stainning showed morphological differences between the motoneurons of each injured group. While the motoneurons of the iT8 animals had polygonal morphology, with a well defined nucleus and nucleolus, which resemble motoneurones of the CNT animals, the iL2 animals motoneurons were heavily stained, adopted a rounded morphology, had a punctuated and irregular pattern of staining and the nucleus and nucleolus did not present a well defined contour.

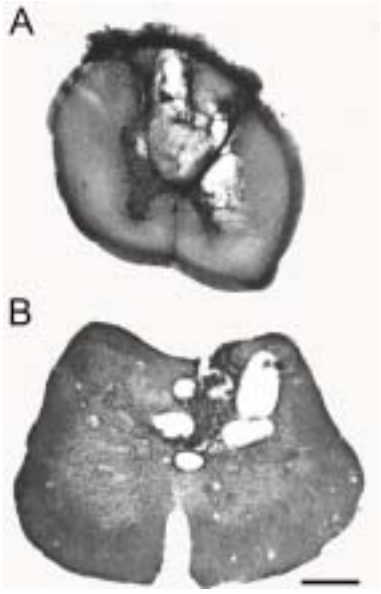

Figure 2. Spinal cord sections stained with cresyil violet at T8 (A) and L2 (B) cord levels. Barr = 500 µ m.

DISCUSION

The results obtained in this work illustrates the importance of the anatomical location of the injury for the development of locomotor deficits. The animals injured in L2 presented gross locomotor deficits compared to mild deficits observed in animals with a similar injury produced at the T8 segment of the spinal cord. The fact that both experimental groups presented similar tissue sparing at the lesion site suggests that the loss of function is not due to differences between the severity of the lesion produced but to its anatomical location. Our results shows a reduction in the motoneuronal survival in both injured groups, and a strong change in the pattern of expression of CGRP in the iL2 animals, compared to the iT8 and CNT group animals. Furthermore, the injuries produced at L2 severely affected the function of the survival motoneurons, inducing a reduction of the MEPs and CMAP amplitudes, and a strong alteration of the H wave response, while the animals injured at T8 showed slight changes in these functions.

Table 1. Electrophysiological results, expressed as the percentage respect to the preoperative values, obtained 14 days after the operation in the iT8 and iL2 experimental groups.

		Tibialis Anterior Muscle		Gastrocnemius Muscles		Plantar Muscle	
	Group	Latency	Amplitude	Latency	Amplitude	Latency	Amplitude
MEPs							
	CNT	91 ± 2,07	118 ± 9,2	97 ± 2,02	100 ± 8,1	91 ± 3,15	128 ± 19,6
	iT8	101 ± 2,77	78 ± 8[a]	103 ± 2,38	68 ± 8.9[b]	102 ± 3,03	71 ± 13,4[b]
	iL2	152 ± 29,9[ad]	6 ± 3,8[cf]	113 ± 6,7[ad]	11 ± 9,5[cf]	206 ± 60[ad]	24 ± 13[ce]
CMAP							
	CNT	97 ± 1,96	102 ± 2,2	101 ± 3,76	101 ± 0,99	95 ± 1,43	101 ± 3,29
	iT8	98 ± 1,87	96 ± 3,47	101 ± 2,89	103 ± 2,50	96 ± 2,35	92 ± 4,84
	iL2	99 ± 1,90	75 ± 8,32[ad]	99 ± 4,60	86 ± 8,09[ad]	102 ± 3,29	62 ± 6,6[ad]
H/M							
	CNT	101 ± 3,50	113 ± 18,9	103 ± 2,94	97 ± 29,1	93 ± 1,86	116 ± 14,6
	iT8	99 ± 2,77	191 ± 43,2	103 ± 5,49	156 ± 22,7	98 ± 1,89	162 ± 18,1
	iL2	109 ± 4,40	158 ± 26,7	117 ± 6,95	94 ± 29,2	101± 3,78	563 ± 92,[ad]

p< 0.05 vs CNT, (b) p< 0.01 vs CNT, (c) p< 0.001 vs CNT, (d) p< 0.05 vs iT8, (e) p< 0.01 vs iT8, (f) p< 0.001 vs iT8

The photochemical injury affected basically the dorsal aspect of the spinal cord which lead to the disruption of the corticospinal and rubrospinal tracts,the dorsal columns, as well as partially the spinocerebellar and some of the serotoninergic projections from the brain stem [18] . The reduction of the MEPs corroborate the injury of these spinal pathways [8] . Magnuson et al., (1999) reported that mild excitotoxic injuries produced in the gray substance of the rostral lumbar enlargement of the rat gave rise to a dramatic loss of the animals locomotor habilities compared to similar injures produced at the mid thoracic spinal cord [11] . The authors suggested that the removal of the neuronal propiospinal circuitry, which constitutes the central pattern generator of locomotion (CPG), was the main responsable of causing these deficits. It is well stablished that the CPG is present at the rostral aspect of the lumbar enlargement of the mammalian spinal cord [3] . However, the locomotor deficits produced by lumbar injuries may not only be due to the ablation of the CPG, and possible changes in the survivance and function of the lumbar motoneuronal pool may take part in this behavioral alteration. Our histological results have shown a significant reduction in the number of cresyl violet neurons in both experimental groups, indicating that some lumbar motoneurons died after the injury. These findings fit with previous studies which shown that lumbar motoneurons death after thoracic spinal cord lesions [6, 14] . In contrast, McBride and Ferringa [13] did not account any lumbar motoneuron death after a complete section of the thoracic spinal cord.

The death of lumbar motoneurons may not be the only cause for the strong reduction in the electrophysiological results obtained in the iL2 group. In addition, the surviving motoneurons may present biochemical and physiological alterations which influence their function. In this sense the iL2 animals showed a reduction in the CMAP amplitude, indicating a reduction of the electrically evoked activity of the muscle. This phenomena could explained by an alteration of the muscle activity and/or by the disfunction of motoneurons induced by the injury. However, the fact that any animal of the iL2 and iT8 groups neither presented muscular atrophy nor weight loss suggests that the reduction of the CMAP may be due to alterations of the motoneurons, and not by changes in the muscle. It is well established that during the “spinal shock” period, motoneurons enter a state of hyperpolarization, which can be maintained for weeks or months until the symptoms drastically change and spasticity appears increasing muscle tone and muscle spasm

[10] . The electrophysiological evidence of these hyperpolarization is the absence of F waves elicited after peripheral stimulation [10] . The causes of this transient motoneuronal hyperpolarization are not fully understood; however, studies in axotomized peripheral nerves have shown changes in the expression of sodium channels in dorsal root ganglia and in spinal sensory neurons that affect the excitability of surviving axons following trauma. The reduction of sodium or potassium channel ratio after injury would inhibit conduction properties. In addition, changes in the electrolytic enviroment induced by the injury may also strongly affects the neuronal function [15] . On the other hand, we have found an increase of the H/M ratio, suggeting an increas in excitability in the motoneurones and/or the strech reflex circuitry. Thompson et al [17] found a mild thoracic contusion increased the lumbar reflex excitability, and enhanced lumbar hyperreflexia. Transection of the spinal cord can enhance monosynaptic transmision at group Ia fiber-motoneuron connections located several segments below the lesion site. The increase in number or amplitude of excitatory afferent synapses enhances the motoneuron discharge, therefore counteracting the hyperpolarization state of the motoneuron [4] .

The functional alteration of the motoneurons has also been proved by the decrease of CGRP immunostaining. The animals of iL2 group presented a strong decrease in the number of CGRP-positive motoneurons, indicating that the survival motoneurones had altered their biochemical properties. Within the spinal cord, motorneurons synthesizes CGRP, which is transported anterogradely to the motor end plate, where it is stored and released. CGRP plays a special role in the maintainance of the the structure and function of the neuromuscular junction. In particular, augments the release of acetylcholine from motor nerve terminals, increases the production of ACh receptors, and regulates ACh phosphorilation [9] . After spinal cord transection, motoneurons below the injury show a decrease in the CGRP immunoreactivity. The loss of supraspinal and propiospinal inputs and/or the abolition of muscle activity causes this diminution [12] .

In summary, the results obtained in this work indicates that the deficits produced by an acute spinal cord injury at L2 are not only due to the damage of the central pattern generator of locomotion, but also to, the death and functional alterations of the lumbar motoneurons worsen the animals outcome. The fact that a high percentage of motoneurons survived to the injury suggests that a rehabilitative therapy would be appropiate for patients with lesions at this spinal segement.

We thank Dr. Rushmore and Dr. Valero-Cabré for fruifull discussions and support. This research was supported by grants from the Ministerio de Sanidad y Consumo (FISss 00/0031-02) and from Ministerio de Ciencia y Tecnología (SAF 2002-04016-C02-02), Spain.

REFERENCES

[1] Adams, R.D., Victor, M. and Ropper A.H., Principles of neurology, McGraw-Hill, New York, 1997, 1227-1235 pp.

[2] Basso, D.M., Beattie, M.S. and Bresnahan, J.C., A sensitive and reliable locomotor rating scale for open field testing in rats, Exp. Neurol., 12 (1995) 1-21.

[3] Cazalets, J.R., Borde, M. and Clarac, F., Localizationand organization of the central pattern generator for hindlimb locomotion in newborn rat, J. Neurosci., 7 (1995) 4943-4951.

[4] Cope, T.C., Hickman, K.R. and Botterman, B.R., Acute effects of spinal transection on EPSPs produced by single homonymus Ia-fibers in soleus motoneurons in the cat, J. Neurophysiol., 60 (1988) 1678-1694.

[5] David, S. and Lacroix. S., Molecular approaches to spinal cord repair, Annu. Rev. Neurosci., 26 (2003) 411-440.

[6] Eidelberg, E., Nguyen, L.H., Poloch, R. and Walden, J.G., Transsynaptic degeneration of motoneurones caudal to spinal cord lesions, Brain Res. Bull., 22 (1989) 39-45.

[7] Fehlings, M.G. and Tator, C.H., The relationships among the severity of spinal cord injury, residual neurological function,

axon counts, and counts of retrogradely labeled neurons after experimental spinal cord injury, Exp. Neurol., 132 (1995) 220-228.
[8] García-Alías, G., Verdú, E., Forés, J., Lopez-Vales, R. and Navarro, X., Functional characterization of photochemical graded spinal cord injury in the rat, J. Neurotrauma, 20 (2003) 501-510.
[9] Ishida-Yamamoto, A. and Tohyama, M., Calcitonin gene-related peptide in the nervous system, Prog. Neurobiol., 33 (1989) 355-386.
[10] Leis, A.A., Kronenberg, M.F., Stetkarova, I., Paske, W.C. and Stokic, D.S., Spinal motoneuron excitability after acute spinal cord injury in humans, Neurology, 47 (1996) 231-237.
[11] Magnuson, D.S.K., Trinder, T.C., Zhang, Y.P., Burke, D., Morassutti, D.J. and Shields, C.B., Comparing deficits following excitotoxic and contusion injuries in the thoracic and lumbar spinal cord of the adult rat, Exp. Neurol., 156 (1999) 191-204.
[12] Marlier, L., Rajaofetra, N., Peretti-Renucci, R., Kachidian, P., Poulat, P., Feuerstein, C., Privat, A., Calcitonin gene-related peptide intensity is reduced in rat lumbar motorneurons after spinal cord transection: a quantitative immunocytochemical study, Exp. Brain Res., 82 (1990) 40-47.
[13] McBride, R.L. and Ferringa, E.R., Ventral horn motoneurons 10, 20 and 52 weeks after T-9 spinal cord transection, Brain Res. Bull., 28 (1991) 57-60.
[14] Nacimiento, W., Sappok, T., Brook, G.A., Toth, L., Schoen, S.W., Noth, J. and Kreutzberg, G.W., Structural changes of anterior neurons and their synaptic input caudal to a low thoracic spinal cord hemisection in the adult rat: a light and electron microscopic study, Acta Neuropathol. 90 (1995) 552-564.
[15] Nashmi, R. and Fehlings, M.G., Mechanisms of axonal dysfunction after spinal cord injury: with an emphasis on the role of voltage-gated potassium channels, Brain Res. Rev., 38 (2001) 165-191.
[16] Rossignol, S., Locomotion and its recovery after spinal injury, Curr. Op. Neurobiol., 10 (2000) 708-716.
[17] Thompson, F.J., Reier, P.J., Lucas, C.C. and Parmer, R., Altered patterns of reflex excitability subsequent to contusion injury of the rat spinal cord, J. Neurophysiol., 68 (1992) 1473-1486.
[18] Tracey, D., Ascending and descending pathways in the spinal cord. In Paxinos, G. (Ed), The rat nervous system. Academic Press, Australia, 1995; pp. 67-80.
[19] Verdú, E., García-Alías, G., Forés, J., Gudiño-Cabrera, G., Muñetón, V.C., Nieto-Sampedro, M. and Navarro, X., Effects of ensheathing cells transplanted into photochemically damaged spinal cord, Neuroreport, 12 (2001) 2303-2309.
[20] Verdú, E., García-Alías, G., Forés, J., Vela, J.M., Cuadras, J., López-Vales, R. and Navarro X., Morphological characterization of photochemical graded spinal cord injury in the rat, J. Neurotrauma, 20 (2003) 483-499